REPRINT NO. 220

R63SD31

CYCLOTRON RESONANCE PROPULSION SYSTEM

D. B. Miller, E. F. Gibbons,
P. Gloersen, and D. J. BenDaniel

SPACE SCIENCES
LABORATORY

MISSILE AND SPACE DIVISION

GENERAL ELECTRIC

ACCESSION for

CFSTI	WHITE SECTION	☑
DDC	BUFF SECTION	☐
UNANNOUNCED		☐

JUSTIFICATION ....

....

BY ....

DISTRIBUTION/AVAILABILITY CODES

DIST.	AVAIL. and/or SPECIAL	
/		

SPACE SCIENCES LABORATORY

AEROPHYSICS SECTION

CYCLOTRON RESONANCE PROPULSION SYSTEM

by

David B. Miller, Edward F. Gibbons, Per Gloersen, and David J. BenDaniel*

*Research Laboratory, Schenectady, N. Y.

Presented at AIAA Electric Propulsion Specialists Conference, Colorado Springs, Colo., March 11-13, 1963

R63SD31
March 1963

MISSILE AND SPACE DIVISION

GENERAL ELECTRIC

CYCLOTRON RESONANCE PROPULSION SYSTEM*

ABSTRACT

A plasma acceleration system is described in which power is transferred from an r-f electromagnetic field to a flowing plasma by means of electron cyclotron resonance coupling. A highly efficient coupling of energy from the r-f field to the plasma can be expected if a right-hand, circularly-polarized wave is used and if the flow conditions of the injected gas are properly established. Characteristics of the plasma stream as it emerges from the resonant magnetic field are predicted by an energy balance analysis which assumes adiabatic invarience. It is for instance shown that a stable, d-c longitudinal electric field should develop as a result of the z-acceleration of the electrons and their resultant separation from the ion component.

Experimental results obtained with a low power (320 watt), S-band (2.45 kmc/sec) microwave accelerator will be presented. Plane rather than circularly polarized waves are used in this system. In spite of this, the coupling of energy into the plasma is found to be quite good, on the order of 80% to 90% efficient. The r-f/plasma interaction zone is rather narrow in this experiment, thereby not making efficient use of the injected gas. As much as 20% of the input power appears in the accelerated plasma stream, however. The effects of magnetic field strength and gas density on exhaust stream characteristics, r-f/plasma interaction zone thickness and r-f reflection coefficient will be described. Design considerations resulting from these experiments and status of a higher-powered, X-band system will be discussed.

*Based upon work performed for the National Aeronautics and Space Administration, Contract NAS 5-1046.

CONTENTS

I. INTRODUCTION

The cyclotron resonance propulsion system under consideration is a device in which a propellant stream is ionized and accelerated by a high frequency electromagnetic field. Principal features of its operation are illustrated by Figure 1. A radio frequency wave is incident upon a flowing gas within a uniform (or slowly diverging) d-c magnetic field. In this interaction region, the direction of r-f field propagation, the stream flow direction and the d-c magnetic field direction are parallel with one another. In addition, the magnetic field strength is adjusted so that electron cyclotron resonance will occur at the r-f field frequency ($\omega = \frac{qe}{m_e} B$), thereby greatly increasing the rate at which energy is transferred from the r-f field to the plasma electrons. After the ionized gas has passed through a certain distance of this interaction region and its electrons have been accelerated to the desired energy (in transverse cyclotron orbits) the gas then enters the diverging portion of the d-c magnetic field where the electron motions are converted from transverse orbits to longitudinal paths out of the accelerator. The charge separation electric field established by the electrons as they escape serves to accelerate the ions longitudinally out of the accelerator. Thus the r-f field force is exerted directly on the electrons, while the ions, coupled to the electrons by the charge separation field, represent the majority of the mass flow.

In this paper both theoretical and experimental phases of the cyclotron propulsion system development program will be presented. In particular are discussed theoretical analyses of the processes by which energy is transferred from the r-f field to cyclotron orbiting of the plasma electrons, and from this transverse electron orbiting to longitudinal motion of the ions. Experimental efforts, primarily concerned with a low-power ($\sim$300 watt), c-w, S-band (2.45 kmc/sec, 12-centimeter) experiment, will also be discussed. Finally, initial steps in the development of a medium power accelerator will be described.

II. PROPAGATION PROBLEM - Transfer of Energy from the Incident R-f Field to the Plasma

In order to evaluate the amount of power which is transferred from an electromagnetic field to a plasma, it is convenient to ascribe medium-like properties to the plasma and then to derive a dispersion relation, giving the propagation constant of the e-m field as a function of its frequency within the medium. In this case, we are interested in the propagation of a right-hand, circularly-polarized wave (i.e., that component of the wave which resonates with the electron cyclotron orbits) into a magnetized plasma. A further restriction is that the propagation vector shall be parallel with the magnetic field. For this situation, one can derive the following expression for the propagation constant k from the electron equations of motion

$$k^2 = \left(\frac{\omega}{c}\right)^2 \left[1 - \frac{\omega_p^2}{\omega^2} \frac{1}{1 - \frac{\omega_c}{\omega} + j\frac{\nu}{\omega}} \right] \tag{1}$$

where $\omega \equiv$ e-m field frequency, radians/second

$\omega_p \equiv$ plasma electron density frequency

$\omega_c \equiv$ electron cyclotron frequency

$\nu \equiv$ electron-ion collision frequency

In as much as a wave of the form $\exp j(kz - \omega t)$ has been assumed in this discussion, damping of the wave, representing power transfer from the wave to the plasma, will be indicated by an imaginary component of k. This also can be described as a real component of the conductivity σ, since, from Maxwell's Equations, one can obtain:

$$\sigma = j\omega\varepsilon_0\left(1 - \frac{k^2c^2}{\omega^2}\right) \tag{2}$$

There are two possible mechanisms by which σ can have a real component. Collisions, represented by the $j\nu/\omega$ term in the denominator of Equation (1), will of course give rise to wave damping. A further source of power absorption arises from Doppler broadening of the resonance due to electrons having a thermal spread in their longitudinal velocities. These power absorption mechanisms are discussed more fully in References 1 and 2.

In the cyclotron resonance accelerator, a flowing plasma situation exists, and in order to make an evaluation of the power which will be absorbed by the plasma, the flow velocity (parallel to the propagation vector) must be taken into account. Two factors may contribute to the flow conditions. In the first place, since the gas is injected longitudinally at the point where r-f power begins to be absorbed and is being pumped away at a downstream location, a flowing situation is immediately established. Secondly, if a magnetic field gradient exists in the r-f/plasma interaction region the electrons will receive an additional increment in longitudinal velocity due to a Lorentz force.

The possible effect of this electron flow is to sweep ionization downstream as fast as it is created and thereby to create a gradual plasma boundary. A simple analysis is for instance given in References 1 and 2 which indicates an exponential electron density build up might be expected. Diffusion of electrons upstream from their point of origin works to destroy this gradual boundary.

A gradual plasma boundary is a desirable characteristic in this device, since such a boundary is significantly less reflecting than an equivalent sharp boundary. In the interests of overall system efficiency, it is desirable to match the plasma and generator as closely as possible, and we have therefore in our experiments tried to incorporate both the injection velocity and field gradient features.

III. MAGNETIC NOZZLE PROBLEM

The energy is initially put into the plasma from the r-f field in the form of transverse electron cyclotron orbiting. The energized plasma must still be extracted through a gradient in the magnetic field before its energy can appear as longitudinal motion. This whole process is predicated on the existence of a longitudinal electric field supported by an unbalance in electron and ion local densities. A derivation will be given here to show characteristics of this charge separation field.

We assume here that time-steady ion and electron streams have relative velocities such that a steady potential hill develops in the exhaust region of the magnetic accelerator. Through this potential sheath the ions are (longitudinally) accelerated. The sheath is maintained by energy extracted from electron motion.

This analysis is based on an energy balance equation as follows:

$$\left(\mathcal{E}_{i\parallel} - \mathcal{E}_{i\parallel o}\right) = \left(\mathcal{E}_{e\perp o} - \mathcal{E}_{e\perp}\right) - \left(\mathcal{E}_{e\parallel} - \mathcal{E}_{e\parallel o}\right) \quad (3)$$

where $\mathcal{E} \equiv$ particle kinetic energy

$i \equiv$ ion

$e \equiv$ electron

$\| \equiv$ parallel to stream direction

$\perp \equiv$ transverse to stream direction

o entrance condition

This expression states that the ion energy gain (in longitudinal motion) equals the electron transverse energy loss minus the electron longitudinal energy gain.

So long as the Debye length is small compared with the longitudinal distance within the sheath over which parameters change significantly, the assumptions can be made that charge neutrality exists and, therefore, that throughout the extraction region the ion and electron particle densities remain approximately equal:

$$n_e \cong n_i \tag{4}$$

From this assumption, continuity then demands that the ion and electron velocities remain approximately equal:

$$v_{e\|} \cong v_{i\|} \tag{5}$$

With this restriction, the following equation may be evolved from the energy equation (3)

$$v_{i\parallel}^2 - v_{o\parallel}^2 = \frac{m_e}{m_i}\left(v_{e\perp o}^2 - v_{e\perp}^2\right) \tag{6}$$

So long as the electron orbits are small in comparison with distances over which the magnetic field changes significantly, the magnetic moment of the electron may be assumed to remain constant (an assumption usually referred to in plasma physics as "adiabatic invariance"). This is expressed as:

$$\frac{v_{e\perp}^2}{B} = \frac{v_{e\perp o}^2}{B_o} \tag{7}$$

where B is the magnetic field strength normal to the orbit plane. Since the electron cyclotron orbits are here transverse to the longitudinal (z) axis, B in Equation (7) may be taken as the z-component of magnetic field strength.

Combining Equations (6) and (7) yields:

$$\mathcal{E}_{i\parallel} = \mathcal{E}_{i\parallel o} + \mathcal{E}_{e\perp o}\left(1 - \frac{B}{B_o}\right) \tag{8}$$

In terms of the sheath potential (referred to plasma potential) this may be rewritten as:

$$\varphi\,(\text{volts}) = \frac{\mathcal{E}_{e\perp o}\,(\text{joules})}{q_e\,(\text{coulombs})}\left(\frac{B}{B_o} - 1\right) \tag{9}$$

What is not included in this analysis is the "microscopic" examination of the electronic motions. It is reasonable to expect that the electrons will, in fact, perform oscillatory motions about their equilibrium positions (in the flowing reference frame). These oscillations will probably be on the order of the electron plasma frequency (i.e., periods much shorter than the transit time of the electrons), but with amplitudes equal approximately to the generalized Debye length (i.e., short in comparison with the extraction sheath thickness).

IV. LOW-POWER, C-W EXPERIMENTS

A. Experimental Apparatus

The experimental studies of the cyclotron resonance propulsion system presented here have been carried out at a low power (320 watts) in the S-band (2.45 kmc/sec) frequency range.

At this frequency, the magnetic field required to obtain electron cyclotron resonance is found to be 870 gauss. This field is produced by a two coil arrangement which not only provides the required resonance field, but which also provides a magnetic mirror to help prevent backstreaming of the plasma against the microwave/vacuum window (see Figure 2).

The source of microwave power is a QK-390 c-w magnetron incorporated into a commercially available circuit package (Raytheon Microwave Power Generator, Model PGM-100). This r-f power is then coupled through the waveguide circuitry to the thrust chamber, where the electromagnetic wave interacts with the flowing gas.

Incident and reflected powers are measured by thermistors mounted in waveguide coupled to the main (generator to thrust chamber) guide in a carefully calibrated reflectometer arrangement. This measurement enabled us to determine the reflection coefficient and, knowing the r-f power generated by the magnetron, to calculate the power transferred to the plasma. No matching arrangement was employed in these low power experiments.

The thrust chamber is a section of waveguide which has one end open to the vacuum system and which has its other end sealed by a dielectric vacuum wall through which the microwave energy can pass. A 1/8" diameter stainless steel tube extending in through the top wall serves as the gas injection nozzle for the thrust chamber (see Figure 2).

Some difficulty was experienced in arriving at a suitable wall material to serve as the sealed end of the thrust chamber. This material must provide a vacuum seal, be transparent to the incident microwave energy, and be able to withstand the high temperature plasma conditions. A satisfactory solution was found by using a .095" thick piece of high purity alumina, and the data presented here was taken with this wall arrangement.

A thermionic filament is generally required in this experiment to initiate the plasma. This filament is a replaceable helix of .015" diameter tungsten wire which is inserted into specially constructed sockets mounted inside the thrust chamber. (See Figure 3 for this and following descriptions). Approximately 10 amperes, at a few volts, are required to bring this filament up to emission temperature. The r-f typically causes something on the order of 100 ma d.c. to flow between this filament and the grounded thrust chamber walls.

The r.f. probes in the thrust chamber are straight wire antennas which protrude a short way into the chamber and which are separated from the plasma by quartz covers. The signals from these probes are rectified by crystal diodes and are then displayed on recording millivoltmeters or sensitive oscilloscopes.

The pendulum-calorimeter consists of a 12.8 gram, 3.1 cm. diameter copper cup cemented to a 1/8" diameter hollow glass rod and supported by brass knife edges. At the top end of the glass rod is a counter balance which enables the pendulum to be quite heavy and yet sensitive to very small forces. Sensitivity is also increased by use of an optical magnifying system to observe deflection. A thermocouple, whose electrical connections are brought through the knife edges, measures the temperatures of the copper cup. The pendulum is calibrated by careful measurement of weight and geometry. The calorimeter is calibrated by the standard techniques of, (1) comparing the thermocouple reading with a calibrated thermometer in a water bath and, (2) measuring the change in temperature of a known water volume due to the emersion of the calorimeter at a known initial temperature. Note that the radial position of the copper cup is adjustable by means of a bellows system.

The E_z probe is a bare wire, two electrode arrangement which samples the difference in potential between two z locations within the plasma in the exit region. When connected to a high impedance voltage measuring instrument such as an oscilloscope, this probe indicates the strength and character of electric fields within the plasma.

B. Experimental Results

During a run, a visible blue cone of plasma is observed to emerge from the thrust chamber into the 12" vacuum chamber. Each run had a duration of from 35 to 90 seconds during which continuous chart recordings of the calorimeter temperature and of two r-f probe voltages and incident and reflected power readings were made. These procedures insured steadiness of operating conditions and comparability of data.

Figures 4 and 5 show the dependence of reflected power and probe #2 signal on axial magnetic field strength and gas density.

At the lowest downstream pressure, 3×10^{-5} mm Hg, no plasma is formed and the transmitted power remains essentially constant throughout the range of magnetic field strength. It will be noted that the reflected power rises at the higher magnetic field strength. This is most likely due to filament current effects as verified by a rise in emission current at these same points.

When the gas flow is increased until the pressure in the test chamber is 1.2×10^{-4} mm Hg, the particle density is sufficient to maintain an intermittent plasma at the high field strength, as indicated by the "splitting" of the reflected and transmitted power curves. Both power readings decrease during plasma conditions and a bright emerging beam is clearly visible in the exhaust region.

Increasing the pressure further stabilizes the high field discharge so that plasma conditions are stable and can be repeatably achieved for magnetic fields in excess of the resonance value of 870 gauss. Again both the transmitted (probe #2) and reflected powers decrease below no plasma conditions, and relatively high power absorption efficiencies are obtained. As the magnetic field is increased, absorption efficiency passes through a maximum at about 1000 gauss, and then begins to decrease at the highest field values. Current limitations on our field coil array prevented us from following this curve further.

At the highest pressure setting shown, 1.9×10^{-4} mm Hg, a second discharge region exists for field strengths of approximately half the value required to initiate lower pressure discharges. This low field plasma could be maintained for field strength varying from 400 to 550 gauss and is characterized by a high reflection coefficient, indicating a highly ionized plasma. The high field plasma was also present and again passed through a maximum before beginning to decrease at the highest field points.

The exhaust stream characteristics were measured by the calorimeter - pendulum. In all cases the copper cup was located on a plane 5-1/2" out from the end of the thrust chamber.

Data were taken for two different gas injection conditions. In the first case the gas was introduced into the thrust chamber at a point 1-1/4" downstream from the microwave/vacuum window, and in the second case the injection point was only 1/4" from the window.

Figures 6 and 7 show the measured plasma stream energy profile for the 1-1/4" injection point.

It is obvious from these figures that the plasma stream is somewhat "hollow", with maximum energy being carried at some non-zero radius. This maximum point appears as a bright cone which is visible within the exhaust stream.

Further conclusions which may be drawn from Figures 6 and 7 are that:

1) Both reflection coefficient and energy efficiency decrease when the magnetic field is increased from 900 gauss (i.e., just above resonance)

to 1050 gauss.

2) Increasing gas flow rate (and therefore also raising downstream pressure) causes the energy efficiency to decrease and the reflection coefficient to become larger.

The thrust density showed some radial dependence and was in general a function of gas density and field strength. It was always on the order of .02 to .04 newtons/m^2. Further thrust data are given below in Table 1.

From thrust and power measurements, the following additional characteristics can be deduced.

1) Overall thrust,
2) Overall plasma stream energy, and therefore overall system efficiency,
3) Stream velocity, and
4) Stream particle density.

An evaluation of the data has been made for one flow setting (~ 10 micro-grams/sec) and one magnetic field strength (900 gauss). The results of this evaluation are shown in Table I.

Figure 3 shows the positions of the r-f probes #1 through #5, with #1 being closest to the waveguide window and to the source of microwave

----

TABLE I

MICROWAVE ACCELERATOR PLASMA STREAM CHARACTERISTICS

R-f frequency	2.45 kmc/second
R-f power (incident)	320 watts
R-f reflection coefficient	0.14
Magnetic field strength	900 gauss
Gas inlet flow rate	$.01 \times 10^{-3}$ grams/second
Downstream gas pressure	2×10^{-4} mm Hg
Gas species	Argon
Gas Injection Point	1 1/4"

Radial Position Inches	Power Density watts/m^2	Thrust Density Newtons/m^2	Velocity m/sec.	Energy per Particle Electron Volts	Particle Density m^{-3}	nv part/ m^2-sec.
0	1.8×10^3	.021	1.7×10^5	6.2×10^3	1.0×10^{13}	1.7×10^{18}
1/4	2.0	.024	1.7	6.2	1.2	2.0
1/2	2.2	.027	1.6	5.5	1.5	2.4
3/4	3.7	.024	3.1	20	.36	1.1
1	5.4	.023	4.7	47	.15	.70
1 1/4	7.7	.024	6.4	87	.09	.56
1 1/2	7.7	.024	6.4	87	.09	.56
2 1/2 (estimate)	2.5	.010	5.0	53	.06	.30

Plasma stream total energy (integrating power density over the estimated curve to 3") $\simeq$ 70 watts.

Estimated overall efficiency $E \simeq \frac{70}{320} \times 100 = 22\%$

Exhaust Flow = $n \times v \times$ Beam cross sectional Area = $.9 \times 10^{15}$

Mass Utilization $\frac{\text{Exhaust Flow}}{\text{Inlet Flow}} = 6\%$

power. Table II lists the ratio of probe signals with and without plasma under various conditions. It is evident from Table II that under none of the recorded conditions did any significant r-f power get to probe #2. It is also evident, however, that with the stronger field a large amount of r-f power was measured by probe #1. The fact that the #1 signal actually increased with plasma in the higher field situation indicates that the major reflecting portion of the plasma existed downstream from probe #1, i.e., between #1 and #2.

It has been theoretically predicted that the reflection coefficient of a plasma will decrease as the plasma boundary becomes more gradual. Thus, from the probe measurements of Table II and the reflection coefficient values given in Figures 5 and 6, we have evidence that the stronger magnetic field causes the plasma boundary to widen and become more gradual. This is possibly due to the "mirror" action of the magnetic field in the region adjacent to the window (see Figure 2). Another important factor no doubt is the fact that close to resonance the energy transfer rate is greatest causing the r-f field to attenuate more rapidly with distance into the plasma. One interesting point that can be made is that little r-f power is actually getting to probe #2 and therefore into the gas flow emerging from the injection nozzle for this 1 1/4" injection point. It appears therefore that the high energy plasma stream is generated from the low density "backwash" gas behind the nozzle, and that, since the mean

TABLE II

MICROWAVE PLASMA ACCELERATOR R-F PROBE CHARACTERISTICS

R-f frequency	2.45 kmc/sec.
R-f power	320 watts

Gas Inlet Flow Rate μg/sec	Downstream Pressure mm Hg	Magnetic Field Gauss	Ratio: plasma/ no plasma rf#1	rf#2	rf#3
~10	2×10^{-4}	900	.014	.016	.01
		1050	1.1	.014	.005
~20	3×10^{-4}	900	.023	.021	0
		1050	2.3	.021	0
~40	4×10^{-4}	900	.29	.013	0
		1050	5.7	.025	0

free path is long, this high velocity ion stream passes undisturbed through the slow moving neutral gas. The most likely explanation as to why the particle energy and therefore the system efficiency were so much higher with the narrow boundary at 900 gauss than with the more gradual transition at 1050 gauss would be that at 900 gauss the field at the boundary was closer to the resonance value. It should also be mentioned that, not only does the accelerator work most efficiently at magnetic field strengths closest to resonance under these conditions, but also best operation is achieved at the lowest gas density at which a steady plasma can be generated.

The most notable differences observed in moving the injection point from 1 1/4" to 1/4" beyond the microwave/vacuum window are outlined in the following paragraphs.

The exhaust beam spreading, as measured in the plane of the pendulum/calorimeter, was reduced by a factor of two.

Figure 8 shows a typical plasma stream energy profile for this operating condition . It will be noted that maximum energy is now contained in the center of the stream rather than at some non-zero radius. Thrust densities, however, generally peaked at some non-zero radius after typically having passed through a dip just off center. This thrust density dip indicates a cone of high velocity particles near the center of the plasma stream. These observations may be seen in Table III which is representative of the exhaust stream characteristics for this injection point.

TABLE III

MICROWAVE ACCELERATOR PLASMA STREAM CHARACTERISTICS

R-f frequency	2.45 kmc/sec.
R-f power (incident)	320 watts
R-f reflection coefficient	0.5
Magnetic Field Strength	1030 gauss
Gas inlet flow rate	$.02 \times 10^{-3}$ grams/sec.
Downstream gas pressure	2.7×10^{-4} mm Hg.
Gas species	Argon
Gas Injection point	1/4"

Radial Position Inches	Power Density watts/m^2	Thrust Density Newtons/m^2	Velocity m/sec.	Energy per Particle Ev	Particle Density m^{-3}	NV $\frac{\text{Particles}}{m^2\text{-sec.}}$
0	5.6×10^3	5.0×10^{-2}	2.2×10^5	11×10^3	1.5×10^{13}	3.5×10^{18}
1/4	5.9	3.6	3.3	23	.5	1.6
1/2	5.8	5.9	2.0	8.5	2.4	4.6
3/4	5.6	4.1	2.8	16	.8	2.2
1	3.7	3.6	2.1	9.1	1.2	2.5
1 1/4	2.2	3.3	1.3	3.7	2.7	3.6

Exhaust Flow = $n \times v \times$ Beam Cross-Sectional Area = 1.6×10^{16} particles/sec.

$$\text{Mass Utilization} = \frac{\text{Exhaust Flow}}{\text{Inlet Flow}} = 5\%$$

Both thrust density and power density are higher, but, since the beam cross-sectional area was reduced by one-fourth, the integrated values of thrust and power were both lower.

The maximum measured efficiency with this configuration was 10%, about one half the maximum efficiency measured for the 1-1/4" injection point; mass utilization was approximately the same as for the 1-1/4" injection position.

Magnetic field dependence was quite different. It was found that at the lower, and more efficient densities, we were unable to generate a continuous plasma under resonance conditions (870 gauss), and it was only at fields of over 1000 gauss that we were able to produce a time-steady plasma beam. Even at the higher densities, where we were able to ignite a discharge at resonant field, it was found to be highly inefficient operation point. One possible explanation for this new behavior is that there was now a pronounced diamagnetic effect which reduced the internal magnetic field to less than the required 870 gauss.

V. MEDIUM-POWER, C-W EXPERIMENTS

Although the low power experiments (described in Section IV above) did demonstrate that a c-w microwave accelerator could generate a steady, energetic plasma stream, it was of interest to get a system into operation at a more reasonable power level before a program of systematic parameter variations was undertaken. For this purpose, we have, therefore,

recently begun tests with an X-band source (8.35 kmc/sec) which will deliver several kilowatts of r-f power. Thrust chamber designs have followed the same general philosophy as used for the low power experiments. The plasma is formed and accelerated in an open-ended cavity, with this cavity in fact being an extension of the waveguide which carries the power from the r-f source. Both metal-walled and dielectric-walled plasma chambers are planned. High temperature dielectrics such as alumina and beryllia are considered necessary in order to achieve any reliable life-time, although initial tests have been performed using quartz containers, in the arrangement shown in Figure 9.
On the order of 25% of the incident power has been recovered by calorimetry in the plasma exhaust stream, and pendulum measurements of this stream indicate thrust densities on the order of 1.5 dynes/cm^2.

REFERENCES

1. P. Gloersen, D. Miller, E. Gibbons, Micorwave Driven Magnetic Plasma Accelerator "Cyclops", Final Report No. 1., Contract No. NAS5-1046, February, 1962.

2. David B. Miller, Per Gloersen, Edward F. Gibbons, David J. BenDaniel, "Cyclotron Resonance Propulsion System", Third Annual Symposium on the Engineering Aspects of Magnetohydrodynamics, University of Rochester, March, 1962.

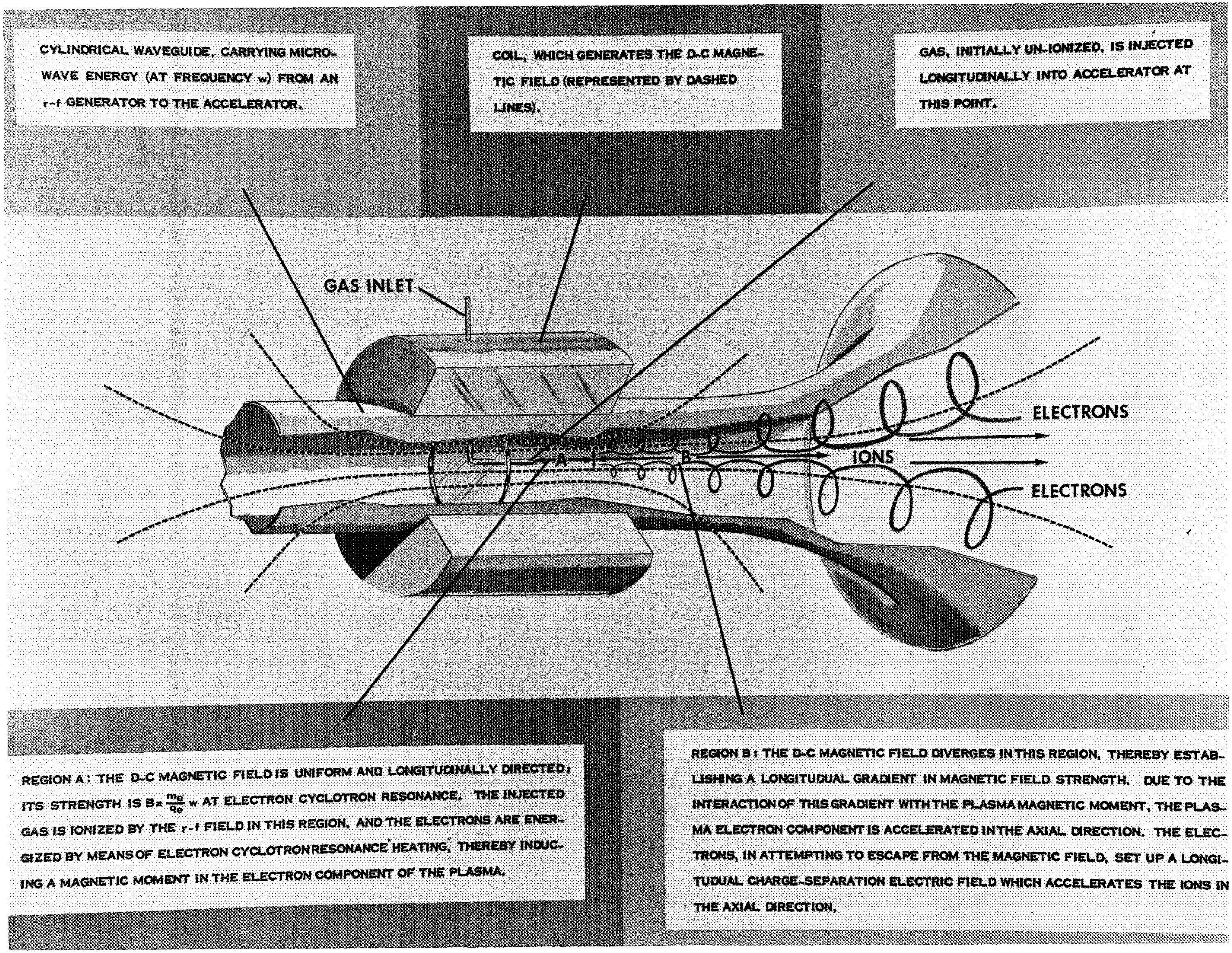
CYLINDRICAL WAVEGUIDE, CARRYING MICRO-WAVE ENERGY (AT FREQUENCY w) FROM AN r-f GENERATOR TO THE ACCELERATOR.
COIL, WHICH GENERATES THE D-C MAGNETIC FIELD (REPRESENTED BY DASHED LINES).
GAS, INITIALLY UN-IONIZED, IS INJECTED LONGITUDINALLY INTO ACCELERATOR AT THIS POINT.
GAS INLET
A
B
ELECTRONS
IONS
ELECTRONS
REGION A: THE D-C MAGNETIC FIELD IS UNIFORM AND LONGITUDINALLY DIRECTED; ITS STRENGTH IS $B = \frac{m_e}{q_e} w$ AT ELECTRON CYCLOTRON RESONANCE. THE INJECTED GAS IS IONIZED BY THE r-f FIELD IN THIS REGION, AND THE ELECTRONS ARE ENERGIZED BY MEANS OF ELECTRON CYCLOTRON RESONANCE "HEATING," THEREBY INDUCING A MAGNETIC MOMENT IN THE ELECTRON COMPONENT OF THE PLASMA.
REGION B: THE D-C MAGNETIC FIELD DIVERGES IN THIS REGION, THEREBY ESTABLISHING A LONGITUDUAL GRADIENT IN MAGNETIC FIELD STRENGTH. DUE TO THE INTERACTION OF THIS GRADIENT WITH THE PLASMA MAGNETIC MOMENT, THE PLASMA ELECTRON COMPONENT IS ACCELERATED IN THE AXIAL DIRECTION. THE ELECTRONS, IN ATTEMPTING TO ESCAPE FROM THE MAGNETIC FIELD, SET UP A LONGITUDUAL CHARGE-SEPARATION ELECTRIC FIELD WHICH ACCELERATES THE IONS IN THE AXIAL DIRECTION.

FIGURE 1.

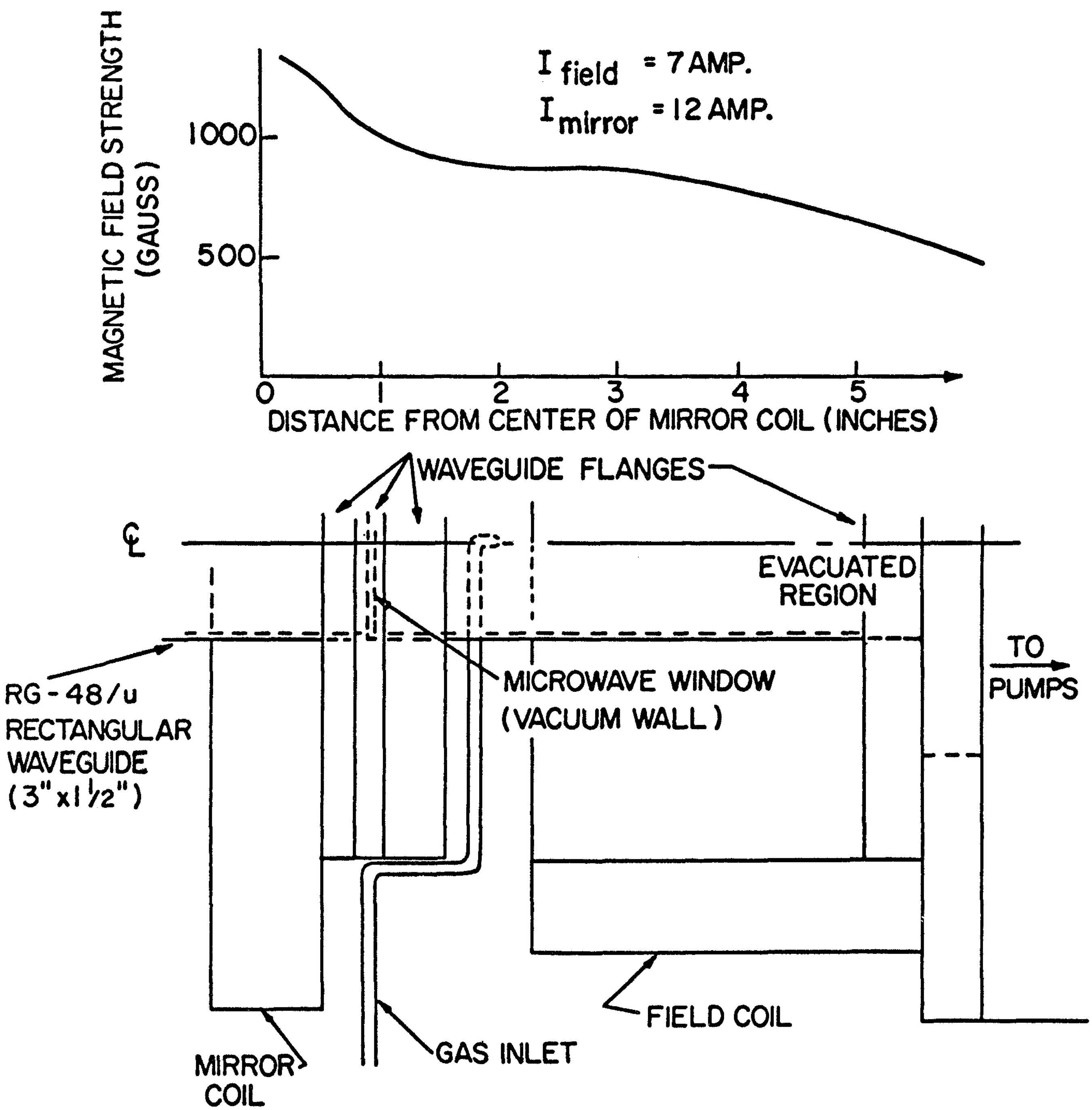

FIGURE 2. METAL-WALLED MICROWAVE PLASMA ACCELERATOR

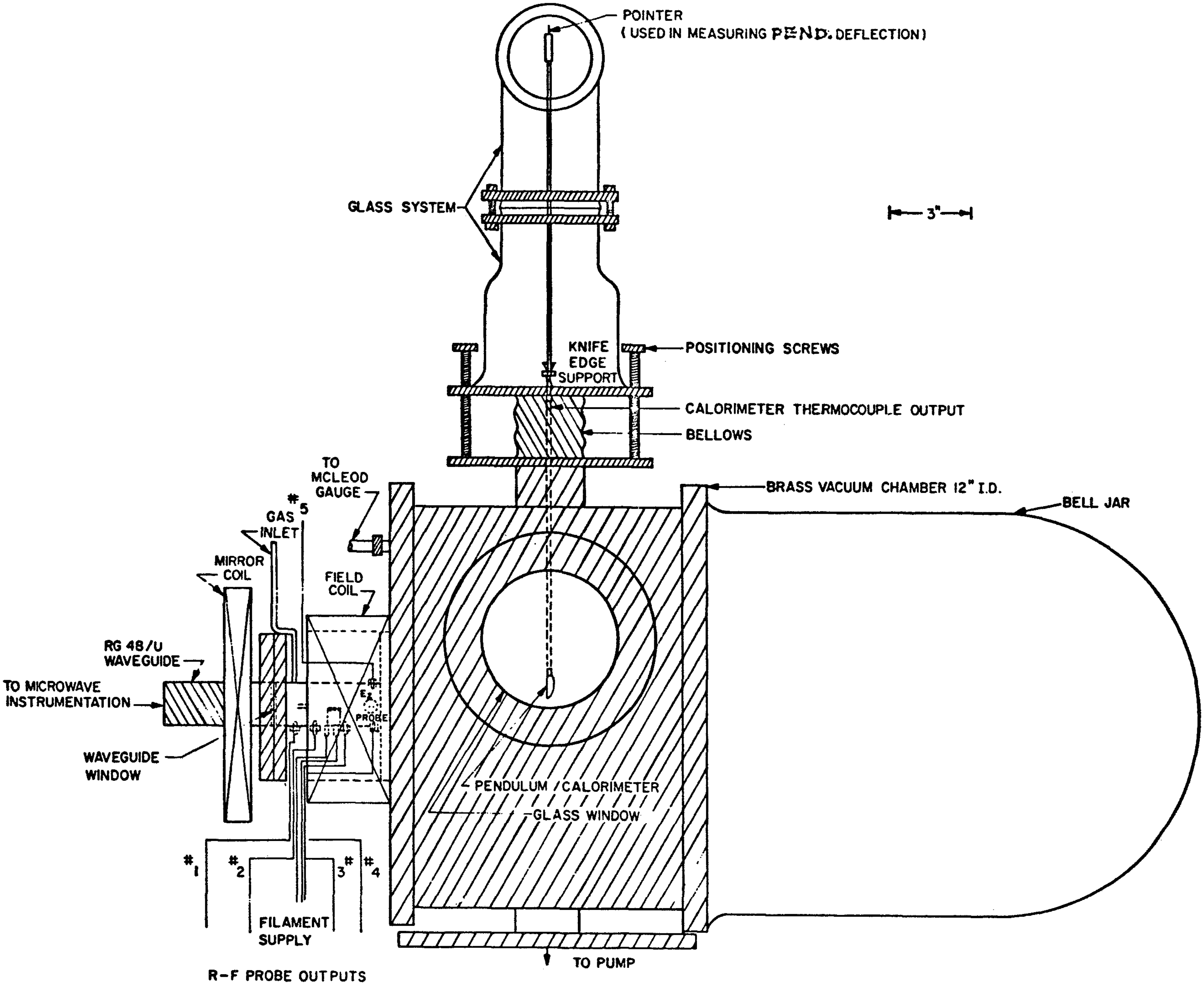

FIGURE 3. METAL-WALLED MICROWAVE PLASMA ACCELERATOR SHOWING INSTRUMENTATION AND VACUUM CHAMBER

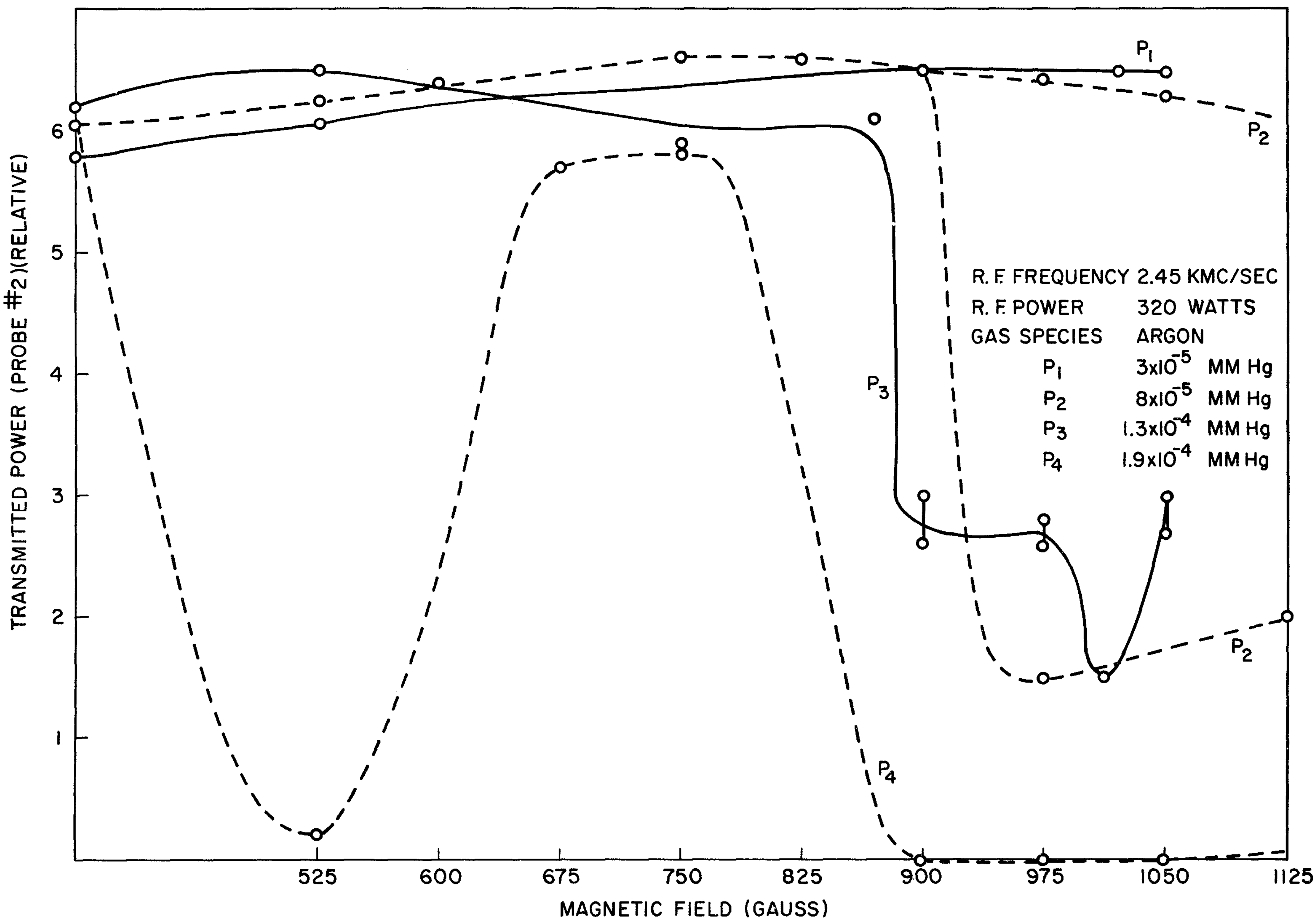

FIGURE 4 R. F. PROBE #2

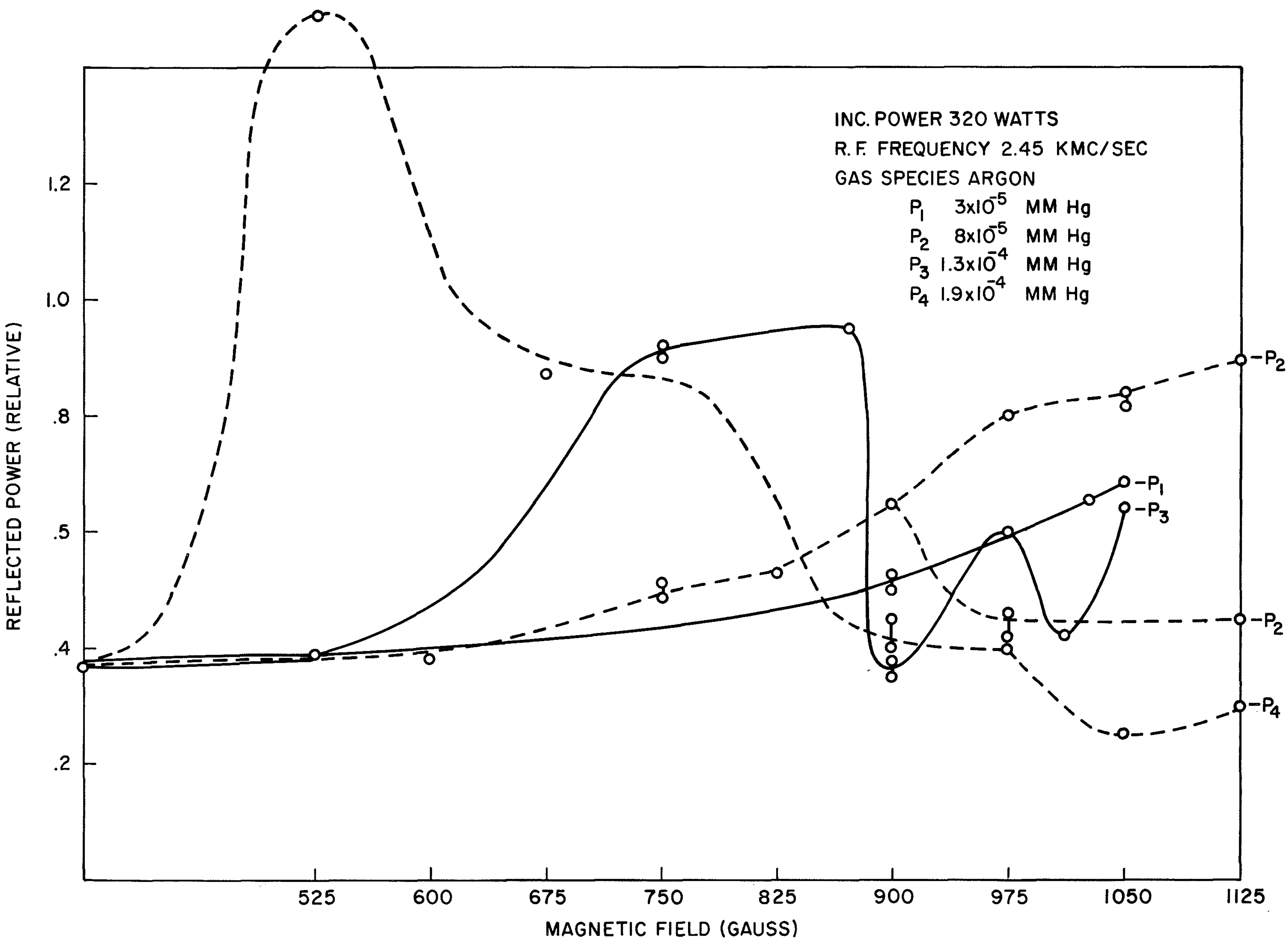

FIGURE 5 REFLECTED POWER VS. MAGNETIC FIELD

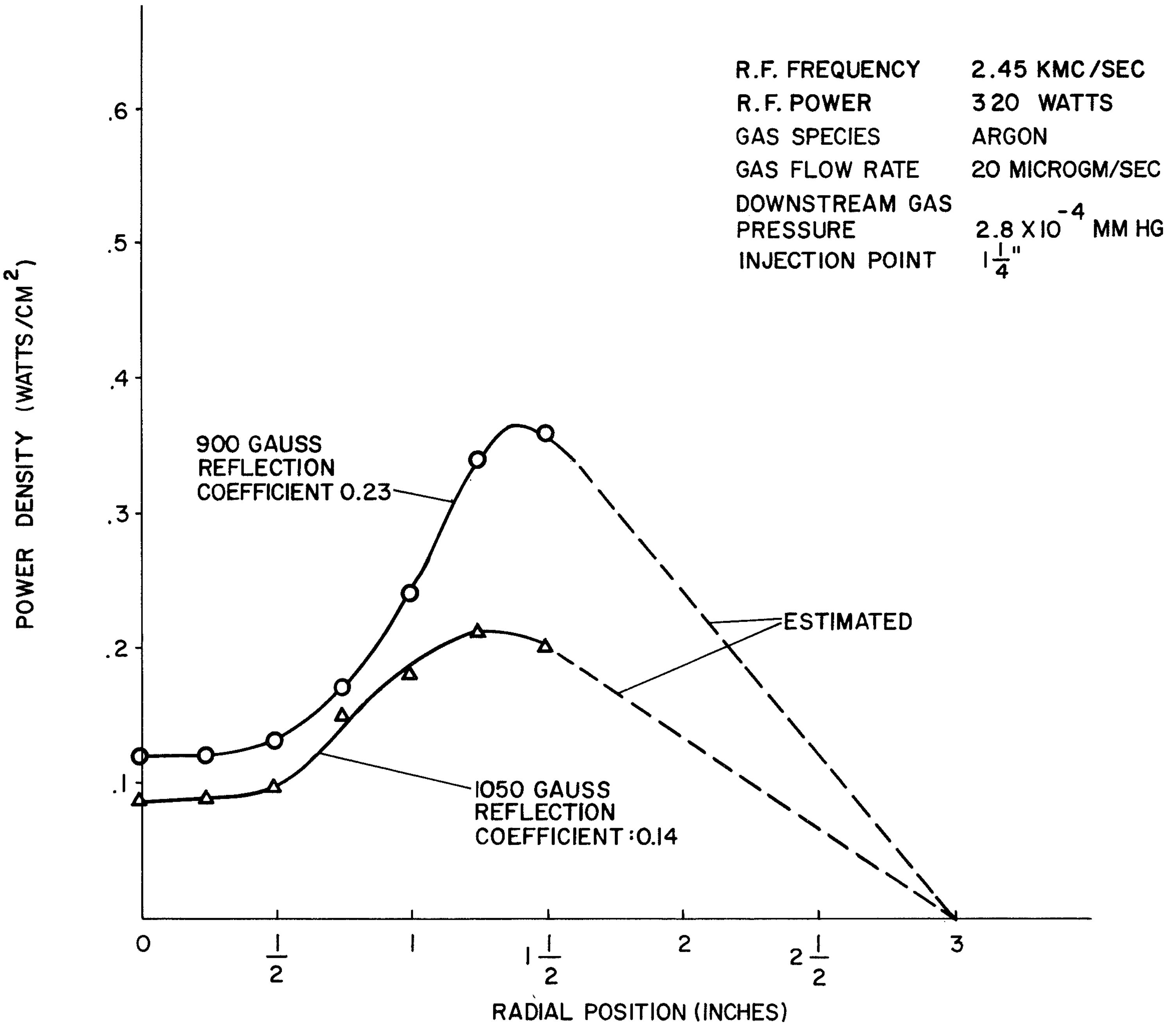

FIGURE 6 MICROWAVE ACCELERATOR PLASMA STREAM ENERGY PROFILE

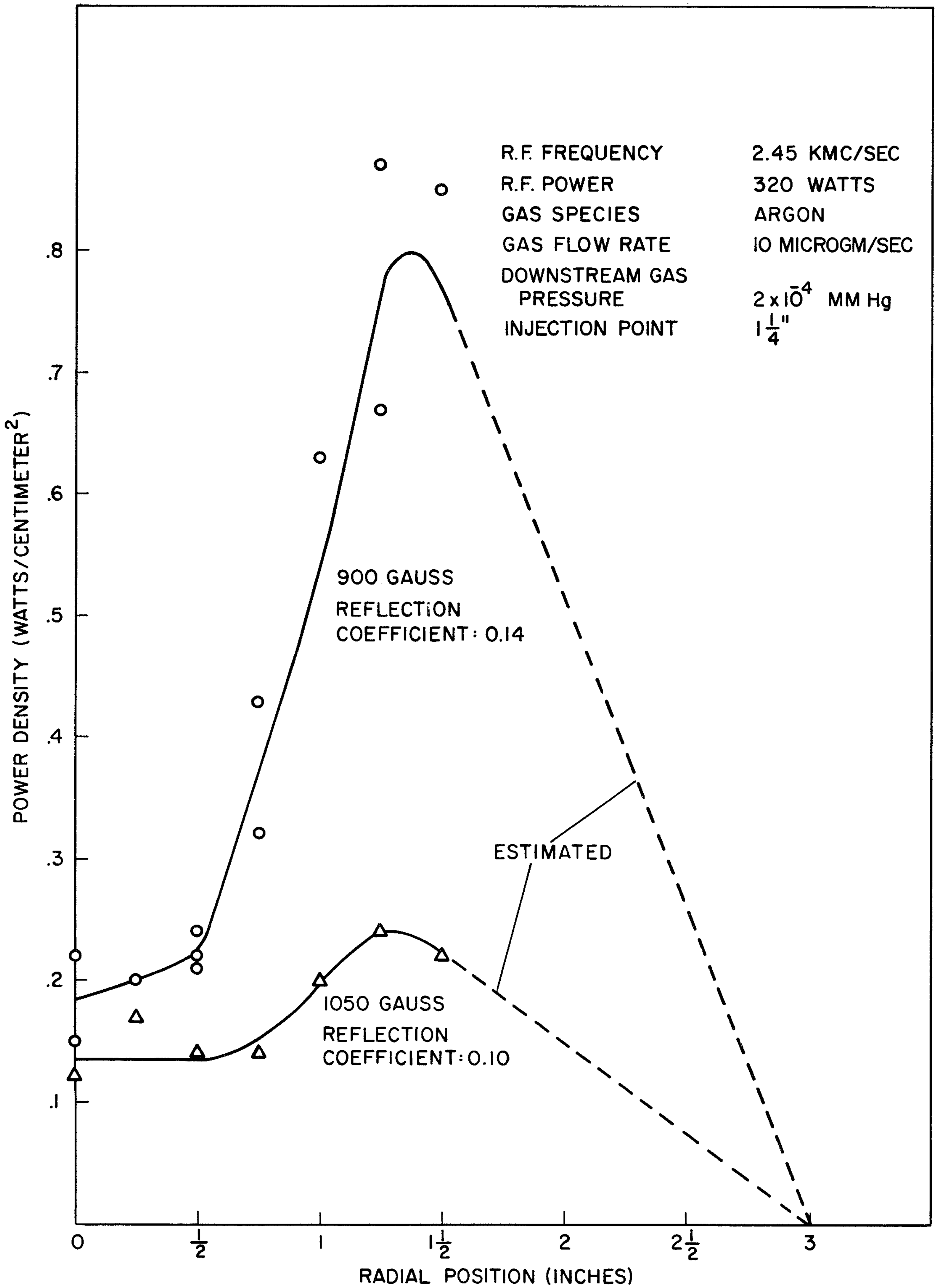

FIGURE 7 MICROWAVE ACCELERATOR PLASMA STREAM ENERGY PROFILE

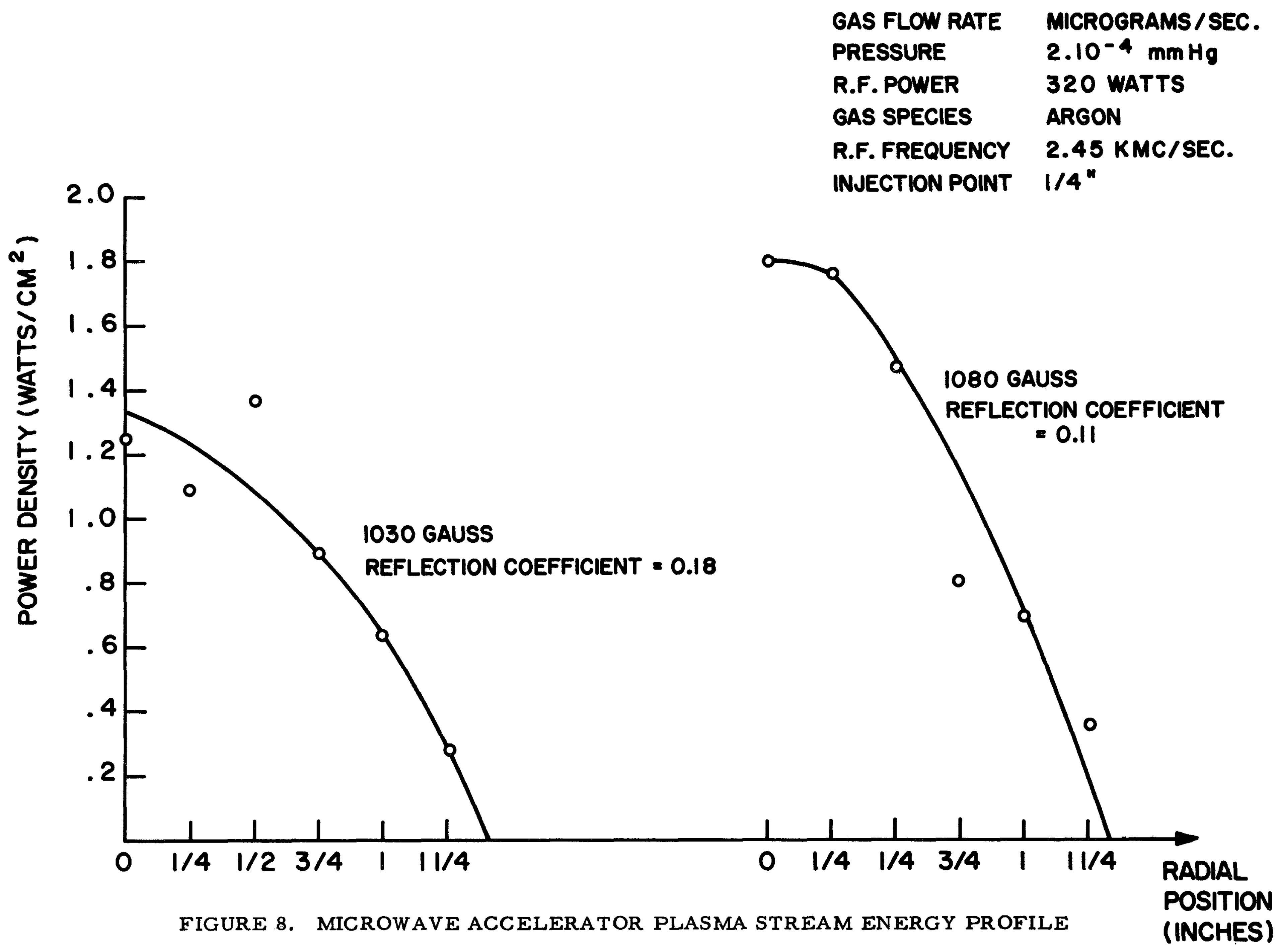

FIGURE 8. MICROWAVE ACCELERATOR PLASMA STREAM ENERGY PROFILE

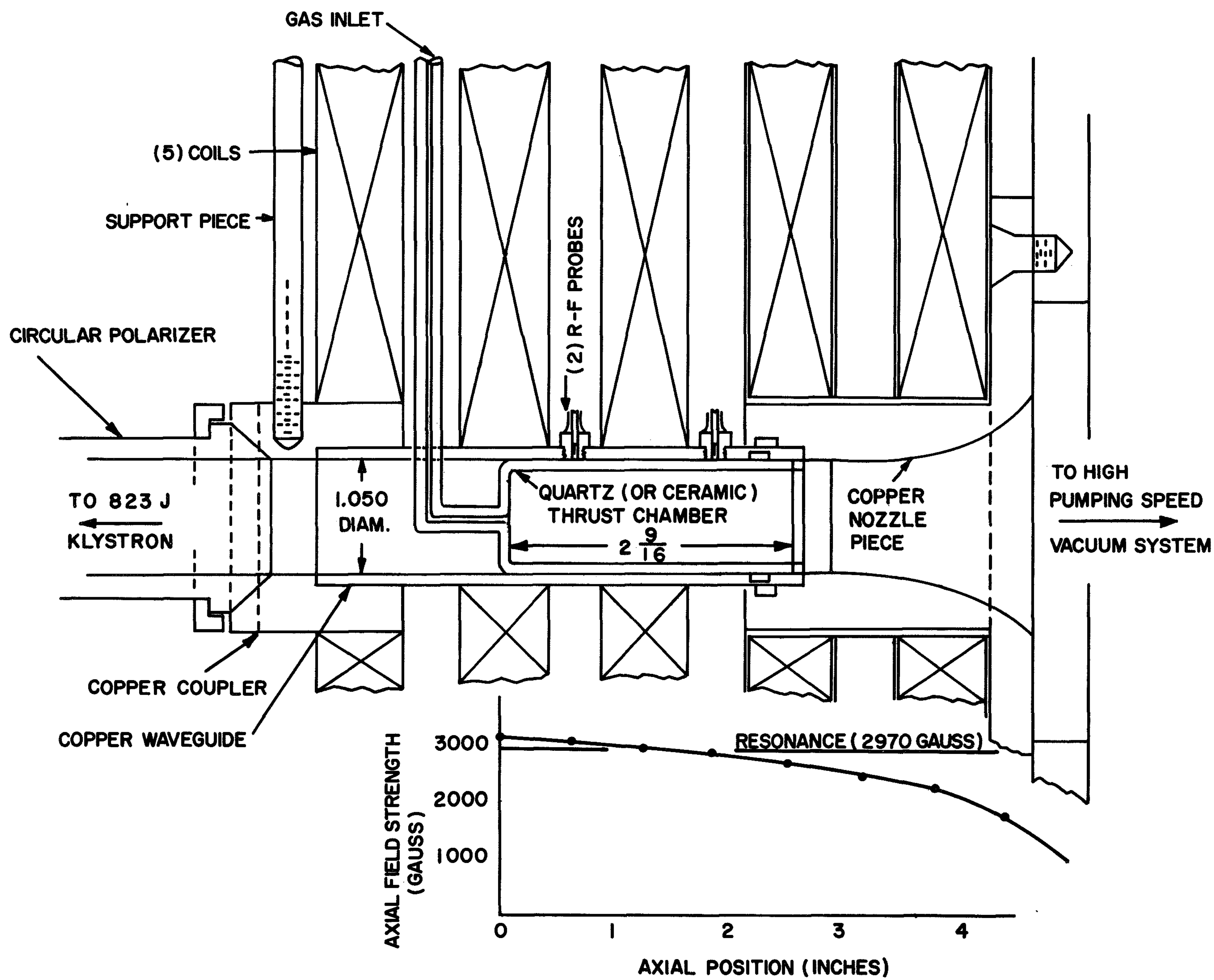
GAS INLET
(5) COILS
SUPPORT PIECE
CIRCULAR POLARIZER
(2) R-F PROBES
TO 823 J
KLYSTRON
1.050
DIAM.
QUARTZ (OR CERAMIC)
THRUST CHAMBER
2 9/16
COPPER
NOZZLE
PIECE
TO HIGH
PUMPING SPEED
VACUUM SYSTEM
COPPER COUPLER
COPPER WAVEGUIDE
RESONANCE (2970 GAUSS)
AXIAL FIELD STRENGTH
(GAUSS)
3000
2000
1000
0
1
2
3
4
AXIAL POSITION (INCHES)

FIGURE 9

Progress Is Our Most Important Product

GENERAL ELECTRIC